Interplays between copper and *Mycobacterium tuberculosis* GroEL1

Dong Yang [1], David P. Klebl [2, 3], Sheng Zeng [1], Frank Sobott [2, 4, 5], Martine Prévost [6], Patrice Soumillion [7], Guy Vandenbussche [6] [#] and Véronique Fontaine [1, #,*]

[1] Microbiology, Bioorganic and Macromolecular Chemistry Unit, Faculty of Pharmacy, Université Libre de Bruxelles (ULB), Brussels, Belgium

[2] The Astbury Centre for Structural Molecular Biology, University of Leeds, Leeds, UK

[3] School of Biomedical Sciences, University of Leeds, Leeds LS2 9JT, UK

[4] School of Molecular and Cellular Biology, University of Leeds, Leeds LS2 9JT, UK

[5] BAMS Research Group, Department of Chemistry, University of Antwerp, Antwerp, 2020, Belgium

[6] Laboratory for the Structure and Function of Biological Membranes, Faculty of Sciences, Université Libre de Bruxelles (ULB), Brussels, Belgium

[7] Biochemistry and Genetics of Microorganisms, Louvain Institute of Biomolecular Science and Technology, Université Catholique de Louvain (UCL), Louvain-la-Neuve, Belgium

[#] Equally contributed

[*] Corresponding author, email: vfontain@ulb.ac.be, postal address: Microbiology, Bioorganic and Macromolecular Chemistry Unit, Faculty of Pharmacy, Université Libre de Bruxelles (ULB), Boulevard du Triomphe, CP205/2, 1050 Brussels, Belgium

28 **Table of contents entry**
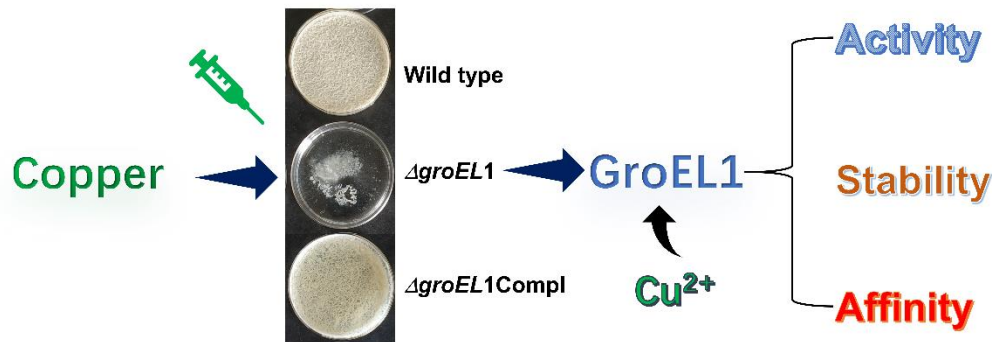
The chaperone GroEL1 enhances copper tolerance during *Mycobacterium bovis* BCG biofilm formation. The binding of copper ions to the GroEL1 histidine-rich region protects the chaperone from destabilization and increases its ATPase activity.

Abstract

The recalcitrance of pathogenic *Mycobacterium tuberculosis*, the agent of tuberculosis, to eradication is due to various factors allowing bacteria to escape from stress situations. The mycobacterial chaperone GroEL1, overproduced after macrophage entry and under oxidative stress, could be one of these key players. We previously reported that GroEL1 is necessary for the biosynthesis of phthiocerol dimycocerosate, a virulence-associated lipid and for reducing antibiotic susceptibility. In the present study, we showed that GroEL1, bearing a unique C-terminal histidine-rich region, is required for copper tolerance during *Mycobacterium bovis* BCG biofilm growth. Mass spectrometry analysis demonstrated that GroEL1 displays high affinity for copper ions, especially at its C-terminal histidine-rich region. Furthermore, the binding of copper protects GroEL1 from destabilization and increases GroEL1 ATPase activity. Altogether, these findings suggest that GroEL1 could counteract copper toxicity, notably in the macrophage phagosome, and further emphasizes that *M. tuberculosis* GroEL1 could be an interesting antitubercular target.

Introduction

Mycobacterium tuberculosis (*M. tuberculosis*) is the causative agent of tuberculosis (TB), a leading infectious disease still causing an estimated 10 million TB cases and 1.4 million deaths in 2018 [1]. This bacterial infection is difficult to treat for various reasons. First, the bacterium has an unusual impermeable cell wall that reduces drug accessibility. The mycobacterial cell wall is composed, from the inside to the outside, of peptidoglycan covalently bound to arabinogalactan which in turn can also be covalently bound to exceptionally long chain fatty acids, mycolic acids. Those are further embedded in an outer membrane, rich in non-covalently bound long fatty acids [2, 3]. Among the non-covalently embedded lipids, phthiocerol dimycocerosates (PDIM), methyl-branched fatty acid-containing lipids, are essential to resist to hostile environment and antibiotics [3-6].

In addition, this pathogen can adopt different strategies to escape bactericidal stress, *e.g.* oxidative stress within macrophages and hypoxia in lung granuloma, among others by entering into a nonreplicating state called dormancy [7-10]. The mycobacterial GroEL1 chaperonin has been previously shown to be essential for metabolic and energetic adaptation under stress, as reflected *in vitro* in a biofilm growth model [11].

M. bovis BCG and *M. tuberculosis* have two *GroEL* encoding genes, *groEL*1 (*Rv3417c*, BCG_3487c) in an operonic arrangement with *groES* (*Rv3418c*, BCG_3488c) and *groEL2* (*Rv0440*, BCG_0479) [12]. They encode two forms of chaperone proteins, GroEL1 (Cpn60.1, Hsp60.1) and GroEL2 (Cpn60.2, Hsp60.2), which are identical between *M. tuberculosis* and *M. bovis*. GroEL1 shares 62 % sequence identity with GroEL2 [12] and 53 % sequence identity and 70% similarity with the well-known *E. coli* GroEL[13]. The *E. coli* GroEL can oligomerize in two heptameric structures stacked back-to-back to promote protein folding with the help of the cochaperonin GroES, in an ATP-dependent manner [14-18]. The divalent cation Mg^{2+} and to a less extent Mn^{2+}, Co^{2+} or Ni^{2+}, has been shown to be required for the *E. coli* GroEL ATPase activity [19]. Interestingly, *M. tuberculosis* GroEL1 has a distinctive histidine-rich C-terminal region, while GroEL2 has a glycine-methionine-rich C-terminal region that is more typical of the GroEL chaperones [12]. In *M. tuberculosis*, both

GroEL proteins are overproduced under stress conditions, including heat shock [20], oxidative stress response [21, 22], osmotic stress [23] and during macrophage infection [24]. The *M. bovis* BCG *groEL*1 knockout mutant shows increased sensitivity to oxidative stress and vancomycin compared to the wild type strain [5]. Furthermore, our previous research demonstrated that the GroEL1 chaperone protein is required for PDIM biosynthesis as the *M. bovis* BCG Δ*groEL1* mutant is devoid of PDIM [5].

Usually, under stress, bacteria use a common virulence and adaptive factor to survive, they form biofilms [13, 22, 25, 26]. Although mycobacterial biofilms were not yet observed in patients with tuberculosis, pathologies involving nontuberculous mycobacteria were shown to be associated with biofilm infections. For pathogenic mycobacteria, biofilm has been shown to be an interesting *in vitro* growth model as, in biofilm, mycobacteria are entering into dormancy and develop adaptative bactericidal escape mechanisms like in *in vivo* stress conditions [27]. For mycobacterial biofilm formation, a high concentration of glycerol (6 % of culture medium) is used and GroEL1 was shown to be required to adapt to this high glycerol concentration [11]. In *in vivo* stress conditions, such as in the macrophage phagosome, the bacilli may encounter additional stress resulting from increased metal ion concentrations [28-30]. Although copper is essential for mycobacteria viability, the high copper ion concentration in host/cell compartments is an efficient antibacterial defence mechanism, especially against the susceptible *M. tuberculosis* [31-33].

The C-terminal histidine-rich region of GroEL1 has been predicted to be involved in metal binding [12]. This was confirmed in the purification process of *M. smegmatis* GroEL1 using Ni-agarose affinity matrix and more recently by isothermal titration calorimetry (ITC) [13, 34]. Given the overproduction of GroEL1 under stresses, we evaluated *M. bovis* BCG biofilm growth in the presence of metal ions and further investigated the impact of metal ions on GroEL1 biochemical characteristics.

Experimental section

Bacterial strains and growth condition

Wild type (wt) *M. bovis* BCG, BCG $\Delta groEL$1 (KO) and BCG complemented (compl) strains were described previously [22]. *M. bovis* BCG was cultured in Middlebrook 7H9 medium (Difco Laboratories) containing 0.05% Tween 80 supplemented with 10% albumin-dextrose complex. The $\Delta groEL$1 strain was grown in a medium with 25 μg/mL kanamycin, and the complemented strain with 25 μg/mL kanamycin and 50 μg/mL hygromycin.

M. bovis BCG biofilm formation

The biofilm cultures were grown on modified Sauton's medium containing 3.5% (v/v) glycerol in the presence or absence of Cu^{2+}, Zn^{2+} or Cd^{2+}. One litre of Sauton's medium contains 0.5 g KH_2PO_4, 0.5 g $MgSO_4$, 2.0 g citric acid, 0.05 g ferric ammonium citrate, 35 mL glycerol, 4.0 g asparagine, 1.435 mg $ZnSO_4$. The pH of the medium was adjusted to pH 7.2 with 1 M NaOH.

To grow biofilms in either 24-well plates or 6 cm diameter polystyrene Petri dishes, 20 μL or 100 μL of precultures (OD_{600} at 0.9-1.0) were inoculated in 2 mL or 10 mL biofilm medium. The dishes or plates were then covered twice with Parafilm® and incubated at 37 °C for 21-28 days without disturbance [27].

Plasmid constructions

The pET-15b vector (Novagen) was modified with a cleavage site for Rhinovirus protease 3C introduced between *Nde*I and *Nco*I in place of the thrombin cleavage site, leaving a sequence encoding a 5×His-tag [35].

The coding sequences corresponding to the *M. tuberculosis* H37Rv *groEL*1*, groEL*2 *and groES* genes were amplified by polymerase chain reaction (PCR). The primers used are shown in supplementary data (**Table S1**). The plasmids *p*MtGroEL1 and *p*MtGroEL1ΔHis were obtained by cloning the PCR products into the modified pET-15b vector, using the restriction sites *Nde*I and *Xho*I. The designed *p*MtGroEL1ΔHis is devoid of the last 30 bases, including the stop codon and 27 bases encoding the last 9 C-terminal amino acid residues, compared with *p*MtGroEL1. Prior to cloning, the modified pET-15b vector was linearized using the restriction enzymes *Nde*I and *BamH*I. The *M. tuberculosis groEL*2 gene was cloned into the modified pET-15b vector using the In-Fusion® HD Cloning Kit (Clontech). The *M. tuberculosis groES* gene was

148 cloned into the modified pET-15b vector dephosphorylated by antarctic
149 phosphatase (Anp), using the *NdeI* restriction site. The plasmids were named
150 *p*MtGroEL2 and *p*MtGroES, respectively. All the plasmid constructions were
151 verified by sequencing.

Protein production and purification

153 The constructed plasmids were transformed into *E. coli* strain BL21(DE3)
154 for protein production. The bacteria were grown in LB medium containing 100
155 μg/mL ampicillin at 37 °C. Gene expression was induced with 1 mM IPTG when
156 the optical density reached 0.5 at 600 nm. Then, the incubation was continued
157 for 20 hours at 18 °C (or 30 °C for GroEL2). The cells were then harvested by
158 centrifugation at 5,000 × g and resuspended in 20 mL of 20 mM HEPES, 300
159 mM NaCl, 20 mM MgSO$_4$, 10 mM imidazole, pH 8.0, EDTA-free protease
160 inhibitor cocktail (Carl Roth) and 10 μg/mL DNase (Sigma).

161 Protein purification was always performed at 4 °C [36]. The resuspended cells
162 were homogenized in a Potter-Elvehjem homogenizer and lysed by four
163 passages through an Emulsiflex-C3 (Avestin). The lysate was collected by
164 centrifugation at 10,000 g and loaded onto a previously equilibrated Poly-Prep
165 column (Bio-Rad) containing 2 mL of Ni-NTA resin (Thermo Scientific). The
166 suspension was incubated for 1 h under gentle agitation. After collecting the
167 column flow-through, the resin was washed with 10 mM and 40 mM imidazole,
168 in 20 mM HEPES (pH 8.0), 300 mM NaCl. The proteins were eluted with 250
169 mM imidazole, 20 mM HEPES (pH 8.0), 300 mM NaCl. Prior to 5 × His-tag
170 cleavage, the buffer was exchanged for 20 mM HEPES, 150 mM NaCl (pH 7.5)
171 on a PD-10 desalting column (GE Healthcare). Then the protein was incubated
172 overnight at 4 °C with protease 3C (protein/enzyme mass ratio of 75:1) for His-
173 tag removal. The protein was further purified on size exclusion chromatography
174 (SEC) using a Superdex 200 10/300 GL analytical column connected to an
175 ÄKTA purifier system (GE Healthcare). The protein solution was eluted with a
176 selected buffer or solution (A: 50 mM Tris-HCl, 150 mM NaCl, pH 7.5 or B: 10
177 mM ammonium acetate, pH 6.9).

178 The purified proteins were flash-frozen in liquid nitrogen and stored at -
179 80 °C. Protein concentrations were determined using the calculated extinction
180 coefficients [37] at 280 nm: 16,960 M^{-1}cm^{-1} for GroEL1 and GroEL1ΔHis, 11,460

181    $M^{-1}cm^{-1}$ for GroES and 15,930 $M^{-1}cm^{-1}$ for GroEL2. The purity and the integrity

182   of recombinant proteins were determined by SDS-PAGE and denaturing mass

183   spectrometry, respectively.

184   **Mass spectrometry**

185   Borosilicate nano-electrospray capillaries (Thermo Scientific) were

186   prepared in-house using a P-97 micropipette puller (Sutter Instrument Co.) and

187   coated with gold/palladium in a Polaron SC7620 sputter coater (Quorum

188   Technologies). Mass spectrometers were operated in positive ion mode.

189   For intact mass determination, proteins were solubilized in a 50 %

190   acetonitrile/1% formic acid (v/v) mixture after being desalted on ZipTipC4

191   (Millipore). Mass spectra were acquired on a Q-TOF Ultima mass spectrometer,

192   typically using a capillary voltage of 1.8-2.0 kV and cone voltage of 50 V. The

193   TOF analyzer was operated in the V mode. Molecular masses were determined

194   after MaxEnt1 deconvolution of the raw m/z data (Waters).

195   For initial metal ion-binding studies, the protein was buffer exchanged into

196   10 mM ammonium acetate pH 6.9 via size exclusion chromatography. Native

197   mass spectra were acquired on a Q-TOF Ultima mass spectrometer (Waters)

198   using the settings described above. The metal binding specificity of proteins

199   was determined, and each protein and metal ion were mixed at a final

200   concentration of 10 μM. Metal ion solutions were prepared using $CoCl_2$, $ZnCl_2$,

201    $NiCl_2$ and $CuCl_2$ salts.

202   Copper-binding was studied more in depth using an Orbitrap Q Exactive

203   Plus UHMR modified for high mass range (Thermo Scientific). The protein was

204   buffer-exchanged via SEC as described above or using two consecutive Zeba

205   spin desalting columns (Thermo Scientific) and used at a final concentration of

206   7.5 μM in 500 mM ammonium acetate pH 6.9. This was found to produce less

207   unfolded protein and allowed copper binding. Typical instrument settings were

208   - 1.7 kV capillary voltage, - 50 V in source trapping, HCD was off and the AGC

209   target set to 106 with a maximum inject time of 500 ms. The mass range was

210   2000 – 20000 m/z to allow detection of high oligomeric species if present. Raw

211   data were analysed and processed using UniDec [38]. $CuCl_2$ was added to the

212   sample to make final concentrations between 1.9 and 30 μM. Similar conditions

213   were used to study the binding of Cd^{2+} to GroEL1.

The effect of copper ion on protein thermal stability

The thermal shift assay in the presence of the fluorescent SYPRO orange dye (Invitrogen) was used to monitor protein stability [39]. The assay was conducted in 96-well plates using the CFX96TM real-time PCR system (Bio-Rad). Briefly, 25 μL of reaction mixture contained 5 μM protein (GroEL1 or GroEL1ΔHis), 0.3 μL of 5000 $\times$ SYPRO Orange, with 10 μM Cu^{2+} in 5 mM HEPES, pH 7.5. The thermocycle parameters were set up as follows: 20 minutes pause at 10 $^{\circ}$C, followed by a melt curve recorded from 10 $^{\circ}$C to 95 $^{\circ}$C, with 1 $^{\circ}$C increase every minute, then pause at 10 $^{\circ}$C for 10 minutes. The fluorescence intensity was recorded at Ex/Em = 465/510 nm. The data were obtained from the Bio-Rad Precision Melt Analysis software 1.0 and exported as Microsoft Excel spreadsheet.

Trypsin digestion susceptibility assay

To investigate the effect of copper ions on protease digestion susceptibility, a trypsin digestion assay was performed as previously described with minor modifications [40] on GroEL1 or GroEL1ΔHis in the presence or absence of Cu^{2+} at 37 $^{\circ}$C. Briefly, the reaction mixture contained 5 μg GroEL1 or GroEL1ΔHis, 0.0015 μg trypsin (a mass ration of protein to trypsin was 10,000:3), in the presence or absence of CuCl$_2$. The reaction was terminated at various times by adding 1.5 μL of 50 mM PMSF and 7.5 μL SDS-PAGE Laemmli buffer (2$\times$) to 6 μL aliquots of the reaction mixture, and the resulting solution was immediately frozen in liquid nitrogen. The samples were finally analysed by SDS-PAGE on a 15 % polyacrylamide gel. In addition, the influence of copper on trypsin activity was evaluated using *Nα*-benzoyl-DL-arginine 4-nitroanilide hydrochloride (BAPNA, Sigma) as substrate [41].

ATPase activity assay

The ATPase activities of the purified recombinant mycobacteria GroEL (GroEL1, GroEL1ΔHis, GroEL2) were quantified using a slightly modified colorimetric assay [42]. Briefly, 100 μL of the reaction buffer containing 10 mM KCl, 2 mM ATP, 10 mM MgCl$_2$, 50 mM Tris-HCl (pH 7.5), 150 mM NaCl, and 10 μM proteins, in the absence or the presence of 20 μM GroES were incubated for 1 hour at 37 $^{\circ}$C. Enzymatic reactions were terminated by addition of 500 μL of 1% SDS. Colour development was measured as follows: 200 μL of

247 ammonium molybdate reagent was added to each tube immediately followed

248 by the addition of 200 μl Elon reagent. After 15 min at room temperature, the

249 absorbance of the final solution (200 μL of reactions in 96 well-plates) was

250 measured at 700 nm. Control experiments without protein were always included.

251 The recombinant *E. coli* GroEL was from Abcam.

252 To investigate the effect of metal ions on ATPase activity, the same

253 experiment was performed in the presence of 100 μM of metal ions (Ni^{2+}, Cu^{2+},

254 Cd^{2+}, Zn^{2+} or Co^{2+}).

255 Structural modelling of GroEL1

256 A BLAST search performed on the Protein Data Bank (PDB) sequences

257 identified GroEL2 from *M. tuberculosis* as a potential template for building a

258 GroEL1 model. Two 3D models of GroEL1 were built by comparative modelling

259 with Modeller 9v11 [43] using the *M. tuberculosis* Cpn60.2 (GroEL2) crystal

260 structure as a template [44] and the sequence alignment carried out with ClustalW.

261 The ATP analogue was positioned based on the superposed GroEL structure

262 (PDB ID: 1SX3) [45] to predict the potential ATP binding site.

263

Results

GroEL1 increases copper tolerance during *M. bovis* BCG biofilm formation

The impact of metal ions was evaluated on the biofilm growth of *M. bovis* BCG strains. As the Δ*groEL1* BCG (KO) strain is more sensitive to glycerol osmotic stress [11], the amount of glycerol in the biofilm culture was reduced to 3.5% (instead of 6%) in order to allow biofilm production by the Δ*groEL1* strain. The wild type (wt) BCG strain was able to form mature biofilm (with ridges and troughs) in the presence of Cu^{2+} concentrations up to 175 μM (**Figure 1**). In contrast, the biofilms of the Δ*groEL*1 strain were already impaired with 100-125 μM Cu^{2+}, showing that loss of GroEL1 enhances mycobacterial susceptibility to copper. Complementation of the *groEL*1 gene in the KO strain fully restored biofilm growth in the presence of Cu^{2+} concentrations up to 175 μM, demonstrating that the loss of GroEL1 is indeed responsible for the enhanced copper susceptibility during biofilm growth (**Figure 1**). This protective effect of GroEL1 was only observed in biofilm culture (Sauton's medium) and not in the planktonic culture (7H9 medium). This could be due to a reduced concentration of free Cu^{2+} concentration in the 7H9 culture, as this medium contains 500 mg/L albumin, well-known to bind Cu^{2+} [46]. Indeed, the minimum inhibitory concentration (MIC) for $CuCl_2$ was identical (150-175 μM) for the three strains in the 7H9 medium.

Does the mutant strain exhibit susceptibility to other metallic ions? To verify this point, biofilm growth was also evaluated in the presence of increasing concentrations of Zn^{2+} and Cd^{2+}. As shown in **Figure S1**, no significant difference in terms of susceptibility to these ions during biofilm growth was observed among the three *M. bovis* BCG strains. Indeed, biofilm cultures were unaffected by Zn^{2+} at concentrations up to 600 μM, which already exceeds the Zn^{2+} concentration inside the infected macrophages [31]. The biofilms of the three

292   strains were similarly affected in Cd^{2+} concentrations > 5 μM. Thus, the GroEL1

293   protein does not seem to protect the bacilli from excessive Cd^{2+}. The GroEL1

294   effect is thus copper specific.

295   **The native histidine-rich region affects GroEL1 stability**

296   To study the role of the C-terminal histidine-rich region (HDHHHGHAH) of

297   GroEL1, the recombinant *M. bovis* BCG proteins GroEL1 and a *M. bovis*

298   GroEL1 devoid of the C-terminal histidine-rich region (GroEL1ΔHis) were

299   purified. These proteins were overproduced in the *E. coli* BL21(DE3) strain,

300   purified by immobilized metal affinity chromatography, treated with human

301   rhinovirus 3C protease for the additional 5×His-tag cleavage, and then further

302   purified by size exclusion chromatography (SEC). The purity and the integrity

303   of recombinant proteins were analysed by SDS-PAGE and mass spectrometry,

304   respectively (**Figure S2**). Mass spectrometry data clearly indicated that the

305   additional N-terminal 5×His-tag was removed in both proteins.

306   Recombinant GroEL1 was eluted in SEC as a single peak but migrated as

307   two bands in SDS-PAGE analysis, i.e. an upper stronger band followed by a

308   weaker band **(Figure S2 A)**. Peptide sequence analysis by mass spectrometry

309   demonstrated that the weak band corresponds to a degradation product of

310   GroEL1 lacking the N-terminal region (about 45 amino acid residues missing

311   out of 543) (data not shown). This proteolysis was not observed for the

312   GroEL1ΔHis, always showing a single band in SDS-PAGE analysis **(Figure S2**

313   **B)**.

314   **GroEL1-copper interaction analysed by native mass spectrometry**

315   To further investigate the interaction between GroEL1 and Cu^{2+}, the metal

316   binding specificity of *M. tuberculosis* GroEL proteins was monitored by native

317   mass spectrometry (**Figure 2**). Native mass spectra were recorded after

318   incubation of the proteins with or without Cu^{2+}. Importantly, the addition of one

319   molar equivalent of Cu^{2+} induced a shift of the GroEL1 peak to a higher m/z

value corresponding to the binding of one atom of copper to the protein (**Figure 2B**). The nearly complete disappearance of the apo peak upon copper addition reflects an effective binding of this metal ion to GroEL1. In contrast, practically no conversion of the apo to the holo form was observed upon addition of one molar equivalent of Cu^{2+} to GroEL1ΔHis (**Figure 2C**). This observation suggests that the Cu^{2+} is mainly bound to the histidine-rich region of GroEL1.

Moreover, the ability of other metal ions (*i.e.* Zn^{2+}, Ni^{2+}, Cd^{2+} and Co^{2+}) to bind to GroEL1 was also assessed (**Figure S3 and S4**). The binding of Zn^{2+} and Ni^{2+} to GroEL1 was also observed but with a lower efficiency than for Cu^{2+} (**Figure S3**). At a metal/protein ratio of 1:1, there were nearly no binding of Cd^{2+} to GroEL1 (**Figure S4**). To further study the copper binding to the protein, GroEL1 was titrated with increasing amounts of Cu^{2+} and analysed by native mass spectrometry (**Figure 3**). Sequential addition of Cu^{2+} led to the appearance of the holo form GroEL1·Cu which was the main population observed at the GroEL1/Cu^{2+} 1:1 molar ratio, as described in the previous experiment. At higher molar ratios, GroEL1·2Cu and GroEL1·3Cu populations were detected with a concomitant decrease of the GroEL1·Cu abundance. On the contrary, in the same range of Cu^{2+} concentrations, the apo form of GroEL1ΔHis did not totally disappear and the highest stoichiometry for the protein/metal complex observed in the presence of four molar equivalents of copper was GroEL1ΔHis·2Cu. For the sake of comparison, the recombinant GroEL2 was also purified (**Figure S2**) and the binding of copper to GroEL2 was also investigated. The binding of copper to GroEL2 gave similar results as the binding of copper to GroEL1ΔHis (**Figure 3**).

The effect of copper on *M. tuberculosis* GroEL1 protein oligomeric state was also investigated by native mass spectrometry (**Figure S5**). The recombinant GroEL1 is mainly monomeric with small amounts of dimeric protein, in agreement with a previous report [47]. The same observations were

348 obtained for the GroEL1ΔHis and GroEL2 (data not shown). Moreover, when

349 adding Cu^{2+}, the overall spectra for GroEL1 and GroEL1ΔHis did not change

350 significantly in the range of 0 to 30 μM $CuCl_2$, indicating that higher oligomers

351 could not be observed under these conditions.

The effect of copper on GroEL1 thermal stability

353 Thermal shift assays were performed to evaluate the effect of Cu^{2+} on

354 protein stability. The use of the SYPRO orange fluorescent dye and a real-time

355 thermocycler to follow thermal denaturation in different conditions enabled the

356 monitoring of GroEL1 and GroEL1ΔHis stability in the presence of Cu^{2+}. In the

357 presence of Cu^{2+} (10 to 50 μM), the Tm values for GroEL1 were higher than for

358 GroEL1ΔHis (**Figure 4**). Although high Cu^{2+} concentrations are deleterious for

359 both proteins, the difference in Tm values suggests that the binding of copper

360 to the histidine-rich region could have a protective effect as the binding of the

361 metal ions is more efficient on GroEL1 than on GroEL1ΔHis.

Protease susceptibility assay

363 To further investigate whether Cu^{2+} could increase the GroEL1 protein

364 stability, a mild trypsin digestion was performed in the absence or the presence

365 of Cu^{2+}. The GroEL1 displayed a higher tolerance to trypsin digestion in the

366 presence of Cu^{2+} (**Figure 5**). In addition, the degree of tolerance increased with

367 the copper concentration (**Figure S6**). The binding of Cu^{2+} to the GroEL1

368 protein improved thus its stability. A similar result was also observed with

369 GroEL1ΔHis (**Figure 5**). A control was performed using *Nα*-benzoyl-DL-

370 arginine 4-nitroanilide hydrochloride (BAPNA) as substrate and demonstrated

371 that the trypsin activity was not affected by the presence of Cu^{2+} and that the

372 protease even displayed a small increase of activity in the range of copper

373 concentrations used in the experiment (data not shown), as previously reported

374 [48]. The fact that the trypsin susceptibility was also decreased for GroEL1ΔHis

375 in the presence of Cu^{2+}, suggests that conformational changes could also occur

376 in the protein upon Cu^{2+} binding to the other coordination sites.

Copper increases the GroEL1 ATPase activity

378 ATP hydrolysis by the recombinant *M. tuberculosis* GroEL proteins was
379 investigated in the presence or absence of metal ions. *M. tuberculosis* GroEL1
380 and GroEL2 displayed weak ATPase activity, with a higher activity for GroEL2
381 than for GroEL1 (**Figure 6**). Surprisingly, the GroEL1ΔHis showed a two-fold
382 increased ATPase activity compared to GroEL1. GroEL1ΔHis and GroEL2 had
383 almost the same activity (**Figure 6**). The presence of GroES, also produced
384 and purified for this study (**Figure S2**), had no impact on GroEL1 and GroEL2
385 *in vitro* ATPase activities, in agreement with previous studies [47, 49]. The GroEL1
386 ATPase activity was increased about eight-fold in the presence of Cu^{2+} (**Figure**
387 **7**). This effect was not observed for GroEL1ΔHis and GroEL2. The other metal
388 ions tested (Ni^{2+}, Co^{2+}, Cd^{2+} or Zn^{2+}) did not influence the GroEL1 protein
389 activity, although the presence of Co^{2+} slightly increased the GroEL1ΔHis and
390 the GroEL2 ATPase activities. The effect of Cu^{2+} and Co^{2+} on recombinant *E.*
391 *coli* GroEL ATPase activity was also evaluated and showed that these metal
392 ions had no effect on its ATPase activity (**Figure S7**).

GroEL1 three-dimensional model

394 To better understand the impact of the histidine-rich C-terminal region on
395 the N-terminal region stability, a GroEL1 three-dimensional structure model was
396 built using the crystal structure of *M. tuberculosis* GroEL2 (PDB ID: 3RTK) [44] as
397 template. Both proteins share 62% sequence identity (86% sequence similarity)
398 in 527 residues overlap. It is worth noting that in the crystal structure of GroEL2,
399 the conformation of the 60 first N-terminal residues and of the 26 last C-terminal
400 residues was not solved, most probably due to the flexibility of these domains.
401 The C-terminal residues are also absent in the published structures of the *E.*
402 *coli* GroEL (*e.g.* PDB ID: 1GRL, 1OEL) [50, 51]. The model of GroEL1 in the
403 present study suggests that the N- and C-terminal domains of the protein could

404   be close to each other in the equatorial domain of the protein (**Figure 8**).

405

Discussion

The GroEL1 protein plays important roles in mycobacterial adaptation to the environment, such as resistance to antibiotic and other various stressful conditions [11, 22, 52]. Copper is on one hand a critical cofactor for various mycobacterial enzymes, including those helping to resist oxidative stress, *i.e.* electron transfer reactions, cytochrome *c* oxidase and Cu/Cu superoxide dismutase, but on the other, high copper concentrations are bactericidal [53, 54].

Our results indicate that high concentrations of Cu^{2+} can reduce *M. bovis* BCG biofilm maturation and that GroEL1 is required to resist to toxic Cu^{2+} concentration under this stress condition. As GroEL1 was unable to protect bacteria against toxic Cd^{2+} concentration, its effect is copper specific. Native mass spectrometry analyses demonstrated the specific binding of copper ions to GroEL1, with a higher affinity for the histidine-rich C-terminal domain. Up to two other binding sites with a lower affinity are most probably present in the protein as deduced from the comparison of the copper binding profiles of GroEL1 and GroEL1ΔHis. The presence of binding sites with different affinities for copper ions was also observed for GroEL1 by isothermal titration calorimetry (ITC) analysis [34].

Ansari *et al*. observed similar results using *M. tuberculosis* strains, however in normal growth condition [34]. They didn't investigate the role of GroEL1 under stress conditions [34]. The fact that they observed an involvement of GroEL1 to mitigate Cu^{2+} toxicity in planktonic growth conditions, which was not detected by our group, could be due either to the use of a different mycobacterium species or to our optimal planktonic growth conditions for *M. bovis* BCG (*i.e.* optimized albumin quality), leading to less GroEL1 production or increased Cu^{2+} capture by our albumin in the 7H9 planktonic cultures [46].

The presence of the Cu^{2+} binding sites on GroEL1 but also the protective role of GroEL1 against high toxic copper concentrations, strongly suggests that this protein could segregate *in vivo* the copper ions present in the macrophage phagosomes [32] and therefore, by decreasing the concentration of free ions, protect bacteria from the bactericidal toxic effect of this metal ion. Usually, copper resistance mechanisms involve copper specific chaperones, storage proteins and efflux systems [55]. In *M. tuberculosis*, various P-type ATPases,

generally induced in stressful conditions, have been reported as possible transporters of heavy-metal cations [56]. For instance, CtpV and CtpC are induced by the intraphagosomal concentrations of Cu^+ and Zn^{2+} [57, 58]. Interestingly, although the *E. coli cop*A gene (ortholog of *ctp*V) encodes two proteins with identical N-terminus, a copper chaperone and a copper transporter [59], neither literature search, nor CtpV/CopA aa Clustal sequence alignment allowed to identify a similar copper chaperone for *M. tuberculosis*. In addition, mycobacterial maintenance of low intracellular Cu concentrations also necessitates MctB, a putative copper transport protein at the outer membrane [60]. The metallothionein MymT, a cysteine-rich protein, able to bind up to six Cu^+, partially involved in copper toxicity resistance, could play the role of a storage protein [61]. Furthermore, a copper inducible *M. tuberculosis* operon, including *lpqS* (encoding a putative lipoprotein), *mmcO* (encoding a mycobacterial multicopper oxidase), *Rv2963* (encoding a possible permease), *mymT* (encoding the metallothionein described above), *socAB* (small ORF induced by Cu A and B) and *ricR* (encoding a repressor of this operon) genes, seems to provide key components of an additional system involved in copper detoxification [30]. All these previously reported mechanisms could help the bacilli to maintain the copper homeostasis in *M. tuberculosis* [30, 62]. However, they seem to lack a key component: a copper chaperone which could shuttle copper to the above mentioned copper binding proteins and efflux pumps [30]. We hypothesized that GroEL1 could possibly function as such a copper-shuttling chaperone, as GroEL1 can be secreted in the culture filtrate [22].

As the recombinant GroEL1ΔHis is less prone to the N-terminal proteolytic degradation during purification (**Figure S2**), we hypothesize that the histidine-rich region in GroEL1 somehow increases the accessibility of the latter to proteolytic enzymes. Although this C-terminal histidine-rich region is involved in GroEL1 destabilisation, the stability of this protein seems improved in the presence of Cu^{2+} binding. Apart from this protective role against higher bactericidal copper concentration, the binding of copper ions to GroEL1 could also have an additional function to improve the GroEL1 N-terminal region stability.

Brazil *et al.* reported that the divalent cations (Ca^{2+}, Mg^{2+}, Mn^{2+}, Zn^{2+}) induce exposure of the *E. coli* GroEL hydrophobic surfaces and strengthen the GroEL hydrophobic binding interactions [63]. This was attributed to a conformation change of GroEL when binding to the divalent cations [64]. Based on our GroEL1 3D model, it is possible that the N- and C-terminal domains of the protein could be close to each other and that the binding of copper ions to the histidine-rich domain could affect the interaction of C-terminal segment with the N-terminal domain thereby reducing the exposure of the latter to proteases. Nevertheless, copper binding is not inducing a modification of the GroEL1 oligomeric state, as demonstrated by native mass spectrometry analysis.

Interestingly, Ansari *et al.*, also built a GroEL1 3D model based on their small angle X-ray scattering (SAXS) data obtained in the presence of various GroEL1/Cu^{2+} ratios [34]. The SAXS analysis suggested that the protein adopts a more open structure in the presence of Cu^{2+} and becomes more flexible. These conformational changes could be responsible for the increase of GroEL1 ATPase activity observed in our study in the presence of copper ions. As the protein is predicted to be more extended and flexible in the presence of Cu^{2+}, it would be expected that GroEL1 would be more susceptible to protease activity. However, this is not what was observed as our limited trypsin digestion assay suggested that GroEL1, especially the N-terminal region, is less accessible to the protease in the presence of Cu^{2+}.

Importantly, the GroEL1 ATPase activity is drastically and specifically increased in the presence of Cu^{2+}, mainly binding to the histidine-rich region. This is only observed for GroEL1 and not for GroEL1ΔHis, GroEL2 and *E. coli* GroEL, suggesting that the binding of copper ions to the GroEL1 histidine-rich C-terminal region induces a conformational change allowing to increase its ATPase activity. This could be due to the GroEL1 stability improvement in the presence of Cu^{2+}. Therefore, in the absence of Cu^{2+}, GroEL1ΔHis and GroEL2, both lacking the histidine-rich region, displayed higher ATPase activity than the GroEL1 possibly because of their higher protein stability. However, in the presence of Cu^{2+}, GroEL1 and GroEL2 show similar ATPase activity.

Conclusions

Here, we propose a novel role for the *M. tuberculosis* GroEL1. This protein could be involved in copper resistance during mycobacterial biofilm formation potentially by acting as a metal storage protein. Therefore, when mycobacteria encounter high copper concentrations, as in the macrophage, GroEL1, by binding copper, could help bacteria to tolerate high copper concentrations and consequently this bactericidal stress.

Conflicts of interest

The authors declare that they have no conflicts of interest with the content of this article.

Acknowledgment

References

1. WHO, Global tuberculosis report, *World Health Organization*, 2019.

2. P. J. Brennan and H. Nikaido, The envelope of mycobacteria, *Annu Rev Biochem*, 1995, **64**, 29-63.

3. M. Jankute, J. A. Cox, J. Harrison and G. S. Besra, Assembly of the Mycobacterial Cell Wall, *Annu Rev Microbiol*, 2015, **69**, 405-423.

4. L. R. Camacho, P. Constant, C. Raynaud, M. A. Laneelle, J. A. Triccas, B. Gicquel, M. Daffe and C. Guilhot, Analysis of the phthiocerol dimycocerosate locus of *Mycobacterium tuberculosis*. Evidence that this lipid is involved in the cell wall permeability barrier, *The Journal of biological chemistry*, 2001, **276**, 19845-19854.

5. K. Soetaert, C. Rens, X. M. Wang, J. De Bruyn, M. A. Laneelle, F. Laval, A. Lemassu, M. Daffe, P. Bifani, V. Fontaine and P. Lefevre, Increased Vancomycin Susceptibility in Mycobacteria: a New Approach To Identify Synergistic Activity against Multidrug-Resistant Mycobacteria, *Antimicrobial agents and chemotherapy*, 2015, **59**, 5057-5060.

6. C. W. Hall and T. F. Mah, Molecular mechanisms of biofilm-based antibiotic resistance and tolerance in pathogenic bacteria, *FEMS Microbiol Rev*, 2017, **41**, 276-301.

7. A. Queiroz and L. W. Riley, Bacterial immunostat: *Mycobacterium tuberculosis* lipids and their role in the host immune response, *Rev Soc Bras Med Trop*, 2017, **50**, 9-18.

8. V. Sundaramurthy, H. Korf, A. Singla, N. Scherr, L. Nguyen, G. Ferrari, R. Landmann, K. Huygen and J. Pieters, Survival of *Mycobacterium tuberculosis* and *Mycobacterium bovis* BCG in lysosomes *in vivo*, *Microbes Infect*, 2017, **19**, 515-526.

9. A. M. Alnimr, Dormancy models for *Mycobacterium tuberculosis*: A minireview, *Braz J Microbiol*, 2015, **46**, 641-647.

548 10. R. D. Turner, C. Chiu, G. J. Churchyard, H. Esmail, D. M. Lewinsohn, N. R.

549 Gandhi and K. P. Fennelly, Tuberculosis Infectiousness and Host Susceptibility,

550 *J Infect Dis*, 2017, **216**, S636-S643.

551 11. S. Zeng, P. Constant, D. Yang, A. Baulard, P. Lefevre, M. Daffe, R. Wattiez

552 and V. Fontaine, Cpn60.1 (GroEL1) Contributes to Mycobacterial Crabtree

553 Effect: Implications for Biofilm Formation, *Front Microbiol*, 2019, **10**, 1149.

554 12. T. H. Kong, A. R. Coates, P. D. Butcher, C. J. Hickman and T. M. Shinnick,

555 *Mycobacterium tuberculosis* expresses two chaperonin-60 homologs,

556 *Proceedings of the National Academy of Sciences of the United States of*

557 *America*, 1993, **90**, 2608-2612.

558 13. A. Ojha, M. Anand, A. Bhatt, L. Kremer, W. R. Jacobs and G. F. Hatfull,

559 GroEL1: A Dedicated Chaperone Involved in Mycolic Acid Biosynthesis during

560 Biofilm Formation in Mycobacteria, *Cell*, 2005, **123**, 861-873.

561 14. C. Chaudhry, G. W. Farr, M. J. Todd, H. S. Rye, A. T. Brunger, P. D. Adams,

562 A. L. Horwich and P. B. Sigler, Role of the gamma-phosphate of ATP in

563 triggering protein folding by GroEL-GroES: function, structure and energetics,

564 *EMBO J*, 2003, **22**, 4877-4887.

565 15. H. S. Rye, A. M. Roseman, S. Chen, K. Furtak, W. A. Fenton, H. R. Saibil

566 and A. L. Horwich, GroEL-GroES cycling: ATP and nonnative polypeptide direct

567 alternation of folding-active rings, *Cell*, 1999, **97**, 325-338.

568 16. T. E. Gray and A. R. Fersht, Cooperativity in ATP hydrolysis by GroEL is

569 increased by GroES, *FEBS Lett*, 1991, **292**, 254-258.

570 17. M. J. Todd, P. V. Viitanen and G. H. Lorimer, Hydrolysis of adenosine 5'-

571 triphosphate by *Escherichia coli* GroEL: effects of GroES and potassium ion,

572 *Biochemistry*, 1993, **32**, 8560-8567.

573 18. P. V. Viitanen, T. H. Lubben, J. Reed, P. Goloubinoff, D. P. O'Keefe and G.

574 H. Lorimer, Chaperonin-facilitated refolding of ribulose bisphosphate

575 carboxylase and ATP hydrolysis by chaperonin 60 (groEL) are K$^+$ dependent,

576 *Biochemistry*, 1990, **29**, 5665-5671.

577 19. G. C. Melkani, G. Zardeneta and J. A. Mendoza, The ATPase activity of

578 GroEL is supported at high temperatures by divalent cations that stabilize its

579 structure, *Biometals : an international journal on the role of metal ions in biology,*

580 *biochemistry, and medicine*, 2003, **16**, 479-484.

581 20. G. R. Stewart, L. Wernisch, R. Stabler, J. A. Mangan, J. Hinds, K. G. Laing,

582 D. B. Young and P. D. Butcher, Dissection of the heat-shock response in

583 *Mycobacterium tuberculosis* using mutants and microarrays, *Microbiology*,

584 2002, **148**, 3129-3138.

585 21. N. S. Dosanjh, M. Rawat, J. H. Chung and Y. Av-Gay, Thiol specific

586 oxidative stress response in Mycobacteria, *FEMS Microbiol Lett*, 2005, **249**, 87-

587 94.

588 22. X. M. Wang, C. Lu, K. Soetaert, C. S'Heeren, P. Peirs, M. A. Laneelle, P.

589 Lefevre, P. Bifani, J. Content, M. Daffe, K. Huygen, J. De Bruyn and R. Wattiez,

590 Biochemical and immunological characterization of a *cpn60.1* knockout mutant

591 of *Mycobacterium bovis* BCG, *Microbiology*, 2011, **157**, 1205-1219.

592 23. Y. Hu, B. Henderson, P. A. Lund, P. Tormay, M. T. Ahmed, S. S. Gurcha,

593 G. S. Besra and A. R. Coates, A *Mycobacterium tuberculosis* mutant lacking

594 the *groEL* homologue *cpn60.1* is viable but fails to induce an inflammatory

595 response in animal models of infection, *Infect Immun*, 2008, **76**, 1535-1546.

596 24. I. M. Monahan, J. Betts, D. K. Banerjee and P. D. Butcher, Differential

597 expression of mycobacterial proteins following phagocytosis by macrophages,

598 *Microbiology*, 2001, **147**, 459-471.

599 25. J. Esteban and M. Garcia-Coca, Mycobacterium Biofilms, *Front Microbiol*,

600 2017, **8**, 2651.

601 26. G. Carter, M. Wu, D. C. Drummond and L. E. Bermudez, Characterization

602 of biofilm formation by clinical isolates of *Mycobacterium avium*, *J Med*

603 *Microbiol*, 2003, **52**, 747-752.

604 27. A. K. Ojha, A. D. Baughn, D. Sambandan, T. Hsu, X. Trivelli, Y. Guerardel, A. Alahari, L. Kremer, W. R. Jacobs, Jr. and G. F. Hatfull, Growth of *Mycobacterium tuberculosis* biofilms containing free mycolic acids and harbouring drug-tolerant bacteria, *Molecular microbiology*, 2008, **69**, 164-174.

608 28. H. Botella, P. Peyron, F. Levillain, R. Poincloux, Y. Poquet, I. Brandli, C. Wang, L. Tailleux, S. Tilleul, G. M. Charriere, S. J. Waddell, M. Foti, G. Lugo-Villarino, Q. Gao, I. Maridonneau-Parini, P. D. Butcher, P. R. Castagnoli, B. Gicquel, C. de Chastellier and O. Neyrolles, Mycobacterial p(1)-type ATPases mediate resistance to zinc poisoning in human macrophages, *Cell Host Microbe*, 2011, **10**, 248-259.

614 29. V. Hodgkinson and M. J. Petris, Copper homeostasis at the host-pathogen interface, *The Journal of biological chemistry*, 2012, **287**, 13549-13555.

616 30. X. Shi and K. H. Darwin, Copper homeostasis in *Mycobacterium tuberculosis*, *Metallomics : integrated biometal science*, 2015, **7**, 929-934.

618 31. D. Wagner, J. Maser, B. Lai, Z. Cai, C. E. Barry, K. Honer zu Bentrup, D. G. Russell and L. E. Bermudez, Elemental Analysis of *Mycobacterium avium*-, *Mycobacterium tuberculosis*-, and *Mycobacterium smegmatis*-Containing Phagosomes Indicates Pathogen-Induced Microenvironments within the Host Cell's Endosomal System, *The Journal of Immunology*, 2005, **174**, 1491-1500.

623 32. F. Wolschendorf, D. Ackart, T. B. Shrestha, L. Hascall-Dove, S. Nolan, G. Lamichhane, Y. Wang, S. H. Bossmann, R. J. Basaraba and M. Niederweis, Copper resistance is essential for virulence of *Mycobacterium tuberculosis*, *Proceedings of the National Academy of Sciences of the United States of America*, 2011, **108**, 1621-1626.

628 33. O. Neyrolles, F. Wolschendorf, A. Mitra and M. Niederweis, Mycobacteria, metals, and the macrophage, *Immunological reviews*, 2015, **264**, 249-263.

630 34. M. Y. Ansari, S. D. Batra, H. Ojha, Ashish, J. S. Tyagi and S. C. Mande, A novel function of *M. tuberculosis* chaperonin paralog GroEL1 in copper

632 homeostasis, *bioRxiv*, 2019, DOI: 10.1101/766162, 766162.

633 35. D. Yang, G. Vandenbussche, D. Vertommen, D. Evrard, R. Abskharon, J.

634 F. Cavalier, G. Berger, S. Canaan, M. S. Khan, S. Zeng, A. Wohlkonig, M.

635 Prevost, P. Soumillion and V. Fontaine, Methyl arachidonyl fluorophosphonate

636 inhibits *Mycobacterium tuberculosis* thioesterase TesA and globally affects

637 vancomycin susceptibility, *FEBS Lett*, 2020, **594**, 79-93.

638 36. C. Structural Genomics, C. China Structural Genomics, C. Northeast

639 Structural Genomics, S. Graslund, P. Nordlund, J. Weigelt, B. M. Hallberg, J.

640 Bray, O. Gileadi, S. Knapp, U. Oppermann, C. Arrowsmith, R. Hui, J. Ming, S.

641 dhe-Paganon, H. W. Park, A. Savchenko, A. Yee, A. Edwards, R. Vincentelli,

642 C. Cambillau, R. Kim, S. H. Kim, Z. Rao, Y. Shi, T. C. Terwilliger, C. Y. Kim, L.

643 W. Hung, G. S. Waldo, Y. Peleg, S. Albeck, T. Unger, O. Dym, J. Prilusky, J. L.

644 Sussman, R. C. Stevens, S. A. Lesley, I. A. Wilson, A. Joachimiak, F. Collart, I.

645 Dementieva, M. I. Donnelly, W. H. Eschenfeldt, Y. Kim, L. Stols, R. Wu, M. Zhou,

646 S. K. Burley, J. S. Emtage, J. M. Sauder, D. Thompson, K. Bain, J. Luz, T.

647 Gheyi, F. Zhang, S. Atwell, S. C. Almo, J. B. Bonanno, A. Fiser, S.

648 Swaminathan, F. W. Studier, M. R. Chance, A. Sali, T. B. Acton, R. Xiao, L.

649 Zhao, L. C. Ma, J. F. Hunt, L. Tong, K. Cunningham, M. Inouye, S. Anderson,

650 H. Janjua, R. Shastry, C. K. Ho, D. Wang, H. Wang, M. Jiang, G. T. Montelione,

651 D. I. Stuart, R. J. Owens, S. Daenke, A. Schutz, U. Heinemann, S. Yokoyama,

652 K. Bussow and K. C. Gunsalus, Protein production and purification, *Nat*

653 *Methods*, 2008, **5**, 135-146.

654 37. M. R. Wilkins, E. Gasteiger, A. Bairoch, J. C. Sanchez, K. L. Williams, R. D.

655 Appel and D. F. Hochstrasser, Protein identification and analysis tools in the

656 ExPASy server, *Methods Mol Biol*, 1999, **112**, 531-552.

657 38. M. T. Marty, A. J. Baldwin, E. G. Marklund, G. K. Hochberg, J. L. Benesch

658 and C. V. Robinson, Bayesian deconvolution of mass and ion mobility spectra:

659 from binary interactions to polydisperse ensembles, *Anal Chem*, 2015, **87**,

660   4370-4376.

661   39. K. Huynh and C. L. Partch, Analysis of protein stability and ligand

662   interactions by thermal shift assay, *Curr Protoc Protein Sci*, 2015, **79**, 28 29 21-

663   28 29 14.

664   40. H. Kawasaki, Y. Kurosu, H. Kasai, T. Isobe and T. Okuyama, Limited

665   digestion of calmodulin with trypsin in the presence or absence of various metal

666   ions, *J Biochem*, 1986, **99**, 1409-1416.

667   41. I. Kurtovic, S. N. Marshall and B. K. Simpson, Isolation and characterization

668   of a trypsin fraction from the pyloric ceca of chinook salmon (*Oncorhynchus*

669   *tshawytscha*), *Comp Biochem Physiol B Biochem Mol Biol*, 2006, **143**, 432-440.

670   42. , Biomembranes. Part Q. ATP-driven pumps and related transport: calcium,

671   proton, and potassium pumps, *Methods Enzymol*, 1988, **157**, 1-731.

672   43. A. Fiser and A. Sali, Modeller: generation and refinement of homology-

673   based protein structure models, *Methods Enzymol*, 2003, **374**, 461-491.

674   44. A. Shahar, M. Melamed-Frank, Y. Kashi, L. Shimon and N. Adir, The

675   dimeric structure of the Cpn60.2 chaperonin of *Mycobacterium tuberculosis* at

676   2.8 Å reveals possible modes of function, *J Mol Biol*, 2011, **412**, 192-203.

677   45. D. K. Clare, P. J. Bakkes, H. van Heerikhuizen, S. M. van der Vies and H.

678   R. Saibil, An expanded protein folding cage in the GroEL-gp31 complex, *J Mol*

679   *Biol*, 2006, **358**, 905-911.

680   46. M. Moriya, Y. H. Ho, A. Grana, L. Nguyen, A. Alvarez, R. Jamil, M. L.

681   Ackland, A. Michalczyk, P. Hamer, D. Ramos, S. Kim, J. F. Mercer and M. C.

682   Linder, Copper is taken up efficiently from albumin and α_2-macroglobulin by

683   cultured human cells by more than one mechanism, *Am J Physiol Cell Physiol*,

684   2008, **295**, C708-721.

685   47. R. Qamra, V. Srinivas and S. C. Mande, *Mycobacterium tuberculosis* GroEL

686   homologues unusually exist as lower oligomers and retain the ability to

687   suppress aggregation of substrate proteins, *J Mol Biol*, 2004, **342**, 605-617.

688 48. H. Steinhart, R. Wieninger-Rustemeyer and M. Kirchgessner, Effect of Cu^{2+}

689 ions on the activity of trypsin on natural substance, *Arch Tierernahr*, 1981, **31**,

690 119-125.

691 49. C. M. Kumar, G. Khare, C. V. Srikanth, A. K. Tyagi, A. A. Sardesai and S.

692 C. Mande, Facilitated oligomerization of mycobacterial GroEL: evidence for

693 phosphorylation-mediated oligomerization, *J Bacteriol*, 2009, **191**, 6525-6538.

694 50. K. Braig, Z. Otwinowski, R. Hegde, D. C. Boisvert, A. Joachimiak, A. L.

695 Horwich and P. B. Sigler, The crystal structure of the bacterial chaperonin

696 GroEL at 2.8 Å, *Nature*, 1994, **371**, 578-586.

697 51. K. Braig, P. D. Adams and A. T. Brunger, Conformational variability in the

698 refined structure of the chaperonin GroEL at 2.8 Å resolution, *Nat Struct Biol*,

699 1995, **2**, 1083-1094.

700 52. A. Sharma, T. Rustad, G. Mahajan, A. Kumar, K. V. Rao, S. Banerjee, D.

701 R. Sherman and S. C. Mande, Towards understanding the biological function

702 of the unusual chaperonin Cpn60.1 (GroEL1) of *Mycobacterium tuberculosis*,

703 *Tuberculosis (Edinb)*, 2016, **97**, 137-146.

704 53. L. Spagnolo, I. Toro, M. D'Orazio, P. O'Neill, J. Z. Pedersen, O. Carugo, G.

705 Rotilio, A. Battistoni and K. Djinovic-Carugo, Unique features of the *sodC*-

706 encoded superoxide dismutase from *Mycobacterium tuberculosis*, a fully

707 functional copper-containing enzyme lacking zinc in the active site, *The Journal*

708 *of biological chemistry*, 2004, **279**, 33447-33455.

709 54. S. K. Ward, B. Abomoelak, E. A. Hoye, H. Steinberg and A. M. Talaat, CtpV:

710 a putative copper exporter required for full virulence of *Mycobacterium*

711 *tuberculosis*, *Molecular microbiology*, 2010, **77**, 1096-1110.

712 55. T. D. Rae, P. J. Schmidt, R. A. Pufahl, V. C. Culotta and T. V. O'Halloran,

713 Undetectable intracellular free copper: the requirement of a copper chaperone

714 for superoxide dismutase, *Science*, 1999, **284**, 805-808.

715 56. L. Novoa-Aponte, A. Leon-Torres, M. Patino-Ruiz, J. Cuesta-Bernal, L. M.

Salazar, D. Landsman, L. Marino-Ramirez and C. Y. Soto, In silico identification and characterization of the ion transport specificity for P-type ATPases in the *Mycobacterium tuberculosis* complex, *BMC Struct Biol*, 2012, **12**, 25.

57. M. A. Forrellad, L. I. Klepp, A. Gioffre, J. Sabio y Garcia, H. R. Morbidoni, M. de la Paz Santangelo, A. A. Cataldi and F. Bigi, Virulence factors of the *Mycobacterium tuberculosis* complex, *Virulence*, 2013, **4**, 3-66.

58. S. K. Ward, E. A. Hoye and A. M. Talaat, The global responses of *Mycobacterium tuberculosis* to physiological levels of copper, *J Bacteriol*, 2008, **190**, 2939-2946.

59. S. Meydan, D. Klepacki, S. Karthikeyan, T. Margus, P. Thomas, J. E. Jones, Y. Khan, J. Briggs, J. D. Dinman, N. Vazquez-Laslop and A. S. Mankin, Programmed Ribosomal Frameshifting Generates a Copper Transporter and a Copper Chaperone from the Same Gene, *Mol Cell*, 2017, **65**, 207-219.

60. A. Senju and G. Csibra, Gaze following in human infants depends on communicative signals, *Curr Biol*, 2008, **18**, 668-671.

61. B. Gold, H. Deng, R. Bryk, D. Vargas, D. Eliezer, J. Roberts, X. Jiang and C. Nathan, Identification of a copper-binding metallothionein in pathogenic mycobacteria, *Nat Chem Biol*, 2008, **4**, 609-616.

62. M. I. Samanovic, C. Ding, D. J. Thiele and K. H. Darwin, Copper in microbial pathogenesis: meddling with the metal, *Cell Host Microbe*, 2012, **11**, 106-115.

63. B. T. Brazil, J. Ybarra and P. M. Horowitz, Divalent cations can induce the exposure of GroEL hydrophobic surfaces and strengthen GroEL hydrophobic binding interactions. Novel effects of Zn^{2+} GroEL interactions, *The Journal of biological chemistry*, 1998, **273**, 3257-3263.

64. D. L. Gibbons and P. M. Horowitz, Ligand-induced conformational changes in the apical domain of the chaperonin GroEL, *The Journal of biological chemistry*, 1996, **271**, 238-243.

Supplementary information

Figure S1. The impact of Zn^{2+} and Cd^{2+} on the various *M. bovis* BCG strains biofilm formation.

Figure S2. Recombinant protein purity and integrity determination.

Figure S3. Native nano-ESI mass spectra of GroEL1 in the absence or presence of Zn^{2+}, Ni^{2+} or Co^{2+}.

Figure S4. Native nano-ESI mass spectra of GroEL1 in the absence or presence of Cd^{2+}.

Figure S5. GroEL1 oligomeric state determination by native mass spectrometry.

Figure S6. Protection of GroEL1 from limited trypsin digestion in a Cu^{2+} concentration dependent manner.

Figure S7. *E. coli* GroEL ATPase activity in the presence of Cu^{2+} and Co^{2+}.

Table S1. Plasmids and oligonucleotide primers.

Figure Legends
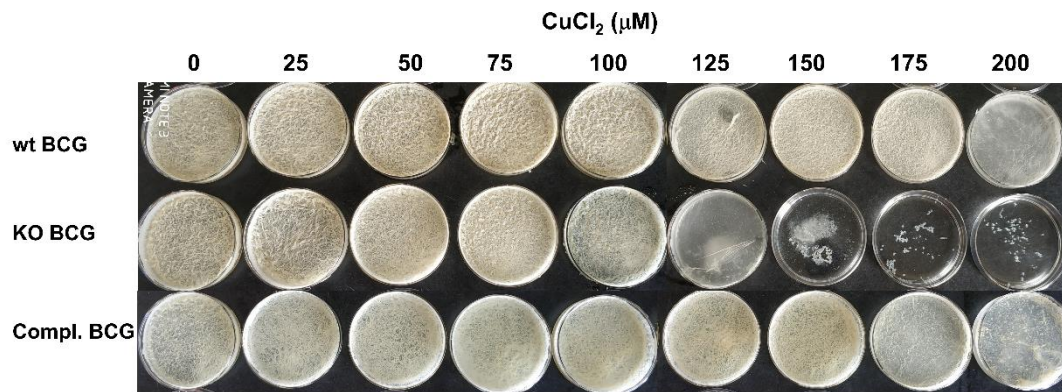
759

760 **Figure 1**. Impact of Cu^{2+} on biofilm formation of various *M. bovis* BCG strains.

761 Biofilm cultures of wild type (wt), $\Delta groEL1$ (KO), KO complemented (compl.) *M.*

762 *bovis* BCG strains were grown in 3.5 % glycerol Sauton's medium in the

763 absence or presence of various concentration of $CuCl_2$ for three weeks. Photos

764 shown are representative of at least three different experiments.

765
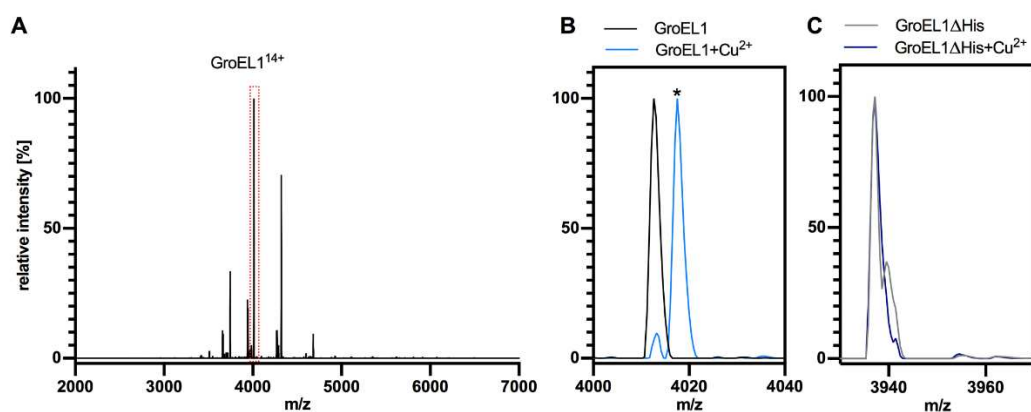
Figure 2. Native nano-ESI spectra of the GroEL1 and the GroEL1ΔHis variant showing different affinities for Cu^{2+}. The protein concentration was 7.5 µM in 500 mM ammonium acetate. (A) Full native mass spectrum of apo GroEL1 shows a narrow charge state distribution with the main charge state $[M + 14H]^{14+}$ highlighted in red. (B) Cu^{2+} binding to GroEL1 shown for the GroEL1^{14+} charge state. A peak shift can be observed upon addition of an equimolar amount of Cu^{2+}, the peak for copper-bound GroEL1 is highlighted with an asterisk. (C) GroEL1ΔHis^{14+} in the presence and absence of one molar equivalent of Cu^{2+}, showing no binding.
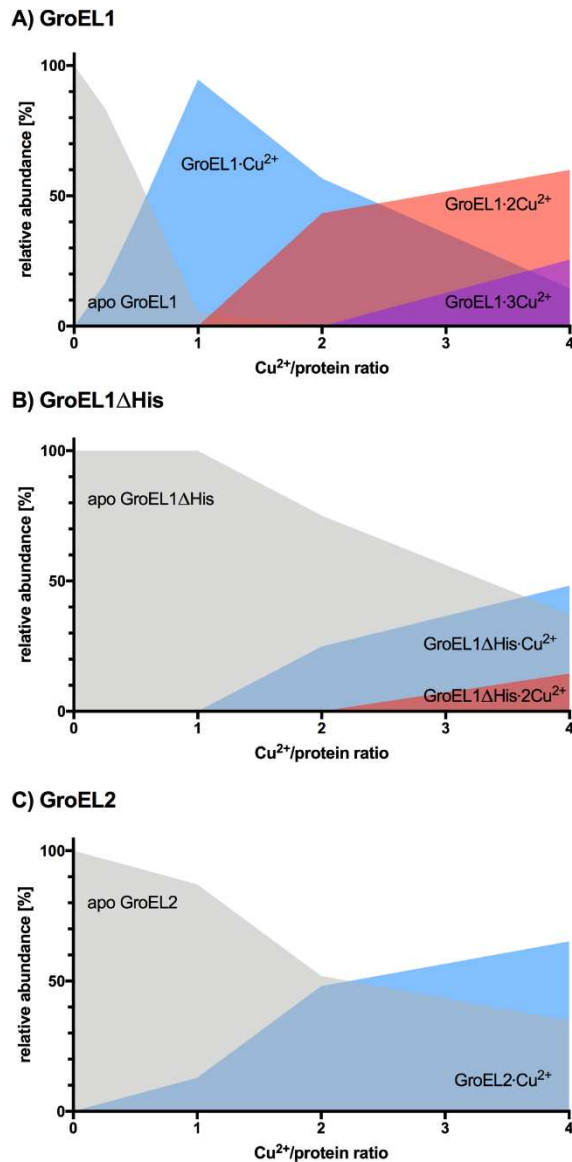
Figure 3. Relative abundance of the different protein-Cu adducts as determined by native mass spectrometry. (A) GroEL1; (B) GroEL1ΔHis; (C) GroEL2. The spectra were recorded at a final protein concentration of 7.5 μM in 500 mM ammonium acetate. Grey, blue, red and purple areas indicate the abundance of apo-protein, 1:1 complex, 2:1 complex and 3:1 complex of protein and Cu^{2+}, respectively. The titration with $CuCl_2$ was performed at molar ratios Cu^{2+} to protein of 0.25:1, 0.5:1, 1:1, 2:1, and 4:1, corresponding to 1.9-30 μM $CuCl_2$. Populations with < 5% intensity are not shown.
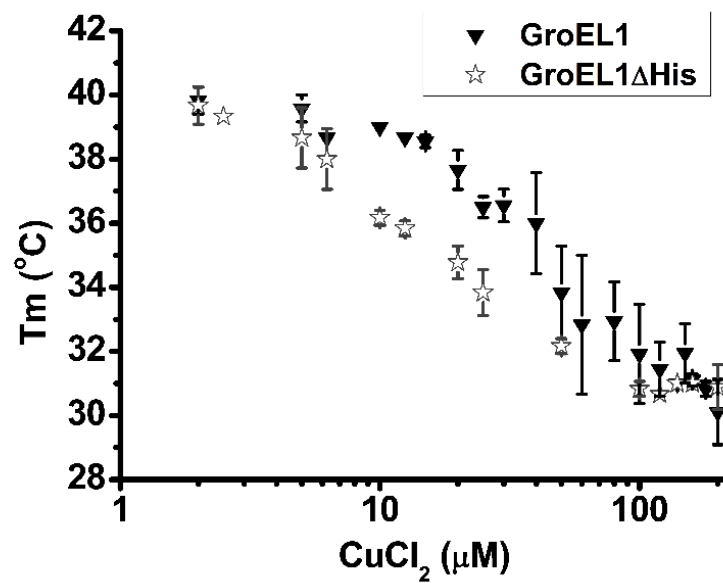
Figure 4. Thermal shift assay to analyse the effect of copper on GroEL1 protein destabilization. The reaction (25 μL) contained 5 μM protein (GroEL1 or GroEL1ΔHis), 0.3 μL of 5000 $\times$ SYPRO Orange, with various concentration of CuCl$_2$ in 5 mM HEPES, pH 7.5. The data correspond to mean and standard deviations and were obtained from three independent experiments.
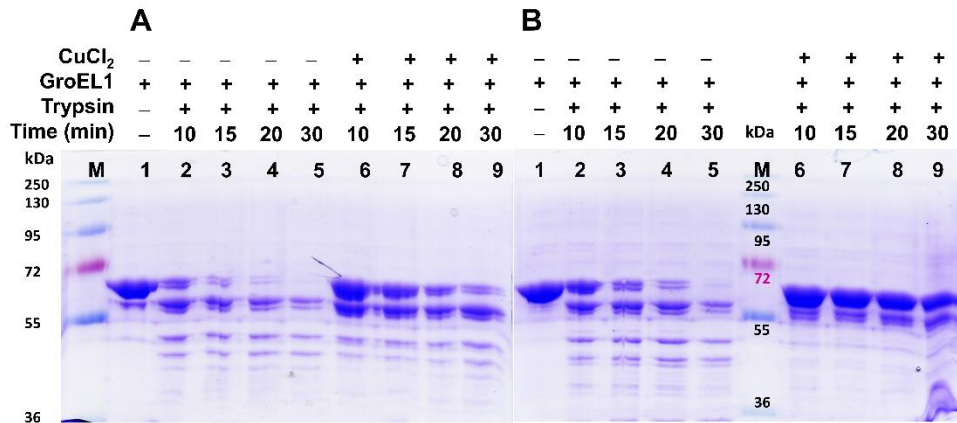
Figure 5. Limited trypsin digestion of GroEL1 (A) and GroEL1ΔHis (B) in the absence or the presence of Cu^{2+}. The reaction was stopped at different times (10, 15, 20, 30 min) by adding PMSF. The reaction products were analysed by 15% SDS-PAGE. Lane M: molecular mass standards; lane 1-9: 5 μg (~9 μM) of GroEL1 (or GroEL1ΔHis); lane 2 to 5: digestion for 10, 15, 20, 30 min, respectively, in the absence of Cu^{2+}; lane 6 to 9: digestion for 10, 15, 20, 30 min, respectively, in the presence of 18 μM Cu^{2+}. The figure is representative of three independent experiments.
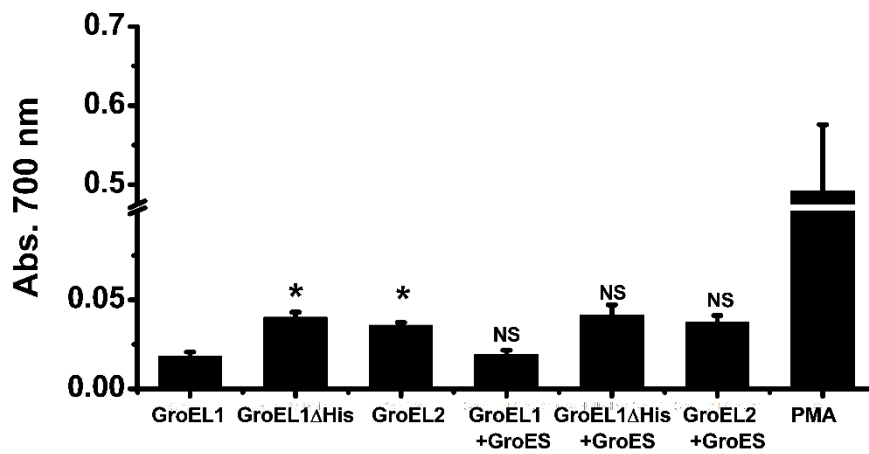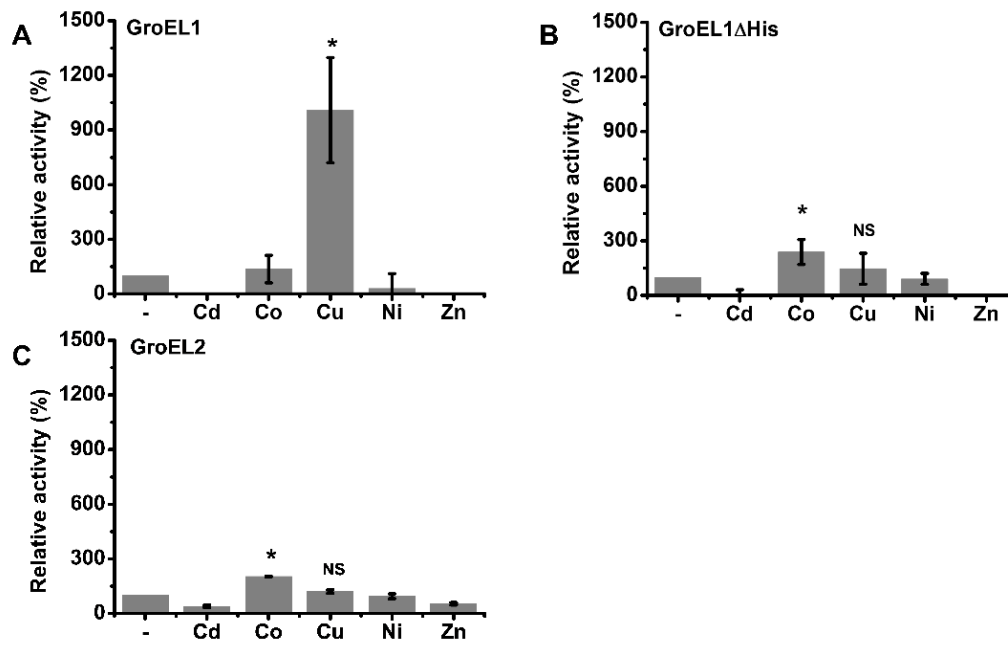
Figure 6. *M. tuberculosis* GroEL protein ATPase activity. Enzymatic reactions were incubated with 10 μM GroEL and 20 μM GroES proteins at 37 °C for 1 h and the absorbance was recorded at 700 nm. Plasma membrane ATPase (PMA) was used as control. The mean from at least three independent experiments for individual data sets was calculated and plotted along with the standard deviation.

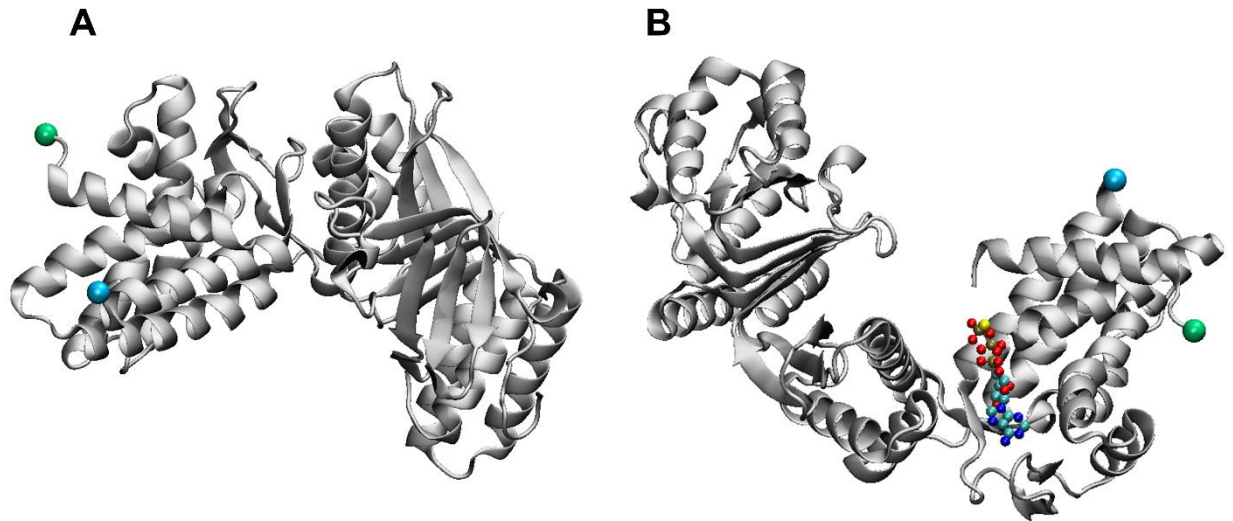**Figure 7.** ATPase activity of 10 μM *M. tuberculosis* GroEL proteins in the presence of 100 μM metal ions. (A) GroEL1, (B) GroEL1ΔHis and (C) GroEL2. The mean from at least three independent experiments for individual data sets was calculated and plotted along with the standard deviation, considering the activity measured in the absence of metal ions as 100%.

A   **B**

821

Figure 8. 3D model of GroEL1 represented as a silver cartoon without (A) or

with ATP analogue (B). The location of an ATP analog (ATPγS) results from the

superposition of the 3D model with the crystal structure of *E. coli* GroEL (PDB

ID: 1SX3). The Cα of the first (residue number 61) and last (residue 518) of the

model are shown as green and blue van der Waals spheres respectively.

827   [1]